THE JOURNAL OF BIOLOGICAL CHEMISTRY VOL. 282, NO. 29, pp. 20941–20947, July 20, 2007

Analysis of a Parallel Branch in the Mitomycin Biosynthetic Pathway Involving the *mitN*-Encoded Aziridine *N*-Methyltransferase*[S]

Received for publication, March 22, 2007, and in revised form, May 15, 2007 Published, JBC Papers in Press, May 16, 2007, DOI 10.1074/jbc.M702456200

Namthip Sitachitta[**], Nicole B. Lopanik[‡§1], Yingqing Mao[**2], and David H. Sherman[‡§¶‖**3]**

*From the [‡]Life Sciences Institute and Departments of [§]Medicinal Chemistry, [¶]Chemistry, and [‖]Microbiology & Immunology, University of Michigan, Ann Arbor, Michigan 48109 and the **Microbiology and Biotechnology Institute, University of Minnesota, Minneapolis, Minnesota 55455*

Mitomycin C is a natural product with potent alkylating activity, and it is an important anticancer drug and antibiotic. *mitN*, one of three genes with high similarity to methyltransferases, is located within the mitomycin biosynthetic gene cluster. An in-frame deletion in *mitN* of the mitomycin biosynthetic pathway was generated in *Streptomyces lavendulae* to produce the DHS5373 mutant strain. Investigation of DHS5373 revealed continued production of mitomycin A and mitomycin C in addition to the accumulation of a new mitomycin analog, 9-*epi*-mitomycin C. The *mitN* gene was overexpressed in *Escherichia coli*, and the histidine-tagged protein (MitN) was purified to homogeneity. Reaction of 9-*epi*-mitomycin C with MitN in the presence of *S*-adenosylmethionine yielded mitomycin E showing that the enzyme functions as an aziridine *N*-methyltransferase. Likewise, MitN was also shown to convert mitomycin A to mitomycin F under the same reaction conditions. We conclude that MitN plays an important role in a parallel biosynthetic pathway leading to the subclass of mitomycins with 9α-stereochemistry but is not involved directly in the biosynthesis of mitomycins A and C.

The mitomycins are a family of antibiotics that are potent alkylating agents upon reductive activation (1–6). One member of the family, mitomycin C (MC)[4] (**3**) (Fig. 1) is an important component of combination chemotherapy for breast, lung, prostate, and colorectal cancer (7–9). However, MC also has detrimental side effects such as myelosuppression and gastrointestinal damage (10). During the past 50 years numerous mitomycin derivatives have been prepared and evaluated in an effort to overcome these clinical limitations (11).

The naturally occurring mitomycins are classified into three groups based on the constituents at the C-9 position as follows: (i) 9β-carbamoylmethyl, (ii) 9α-carbamoylmethyl, and (iii) 9-methylene (Fig. 1). Within these groups, the structures are further differentiated by the substituents at C-7, C-9a, and N-1a. Precursor incorporation experiments demonstrated that the mitosane skeleton is derived from the coupling of 3-amino-5-hydroxybenzoic acid (12) and D-glucosamine (13). Similarly, feeding experiments also revealed that the carbamoyl group at C-10 arises from L-arginine or L-citrulline (14), whereas the *N*- and *O*-methyl moieties originate from L-methionine (15). Although the biosynthetic origin of the mitomycins was revealed over two decades ago, the specific order of assembly leading to this family of natural products remains largely unknown. Recently, we reported the identification and analysis of the mitomycin biosynthetic gene cluster from *Streptomyces lavendulae* NRRL 2564 (16). This particular organism produces mitomycins C and A, as well as smaller amounts of mitomycin B (Fig. 1). It has been suggested that mitomycin A may be the direct precursor of mitomycin C because mitomycin A was found as the predominant compound in earlier stages of fermentation, but its concentration decreases in later stages, whereas the concentration of mitomycin C increases (2).

To unravel the downstream tailoring steps of mitomycin biosynthesis, we have focused on the roles of three *S*-adenosyl-L-methionine (AdoMet)-dependent methyltransferases (encoded by *mmcR*, *mitM*, and *mitN*) identified previously in the mitomycin biosynthetic gene cluster (16). MmcR shows high sequence similarity to a number of methyltransferases that are associated with gene clusters involved in the biosynthesis of phenol-containing compounds such as puromycin and calicheamycin (17, 18). The role of MmcR in installing the 7-*O* methyl groups of mitomycins A and B has been verified through *in vivo* and *in vitro* studies (19). In contrast to MmcR, sequence analysis indicates that MitM and MitN are similar to D-glucose *O*-methyltransferases associated with indolocarbazole natural products (*e.g.* AtmM: 36% identity, 52% similarity (20); RebM: 36% identity, 50% similarity (21, 22)) and other natural product *O*-methyltransferases such as aver-

* This work was supported by National Institutes of Health (NIH) Grant CA/GM81172 and the John G. Searle professorship (to D. H. S.). NMR instrumentation was provided with funds from the National Science Foundation (BIR-961477) and the University of Minnesota Medical School. The costs of publication of this article were defrayed in part by the payment of page charges. This article must therefore be hereby marked "*advertisement*" in accordance with 18 U.S.C. Section 1734 solely to indicate this fact.

[S] The on-line version of this article (available at http://www.jbc.org) contains supplemental Fig. 1 and Table 1.

[1] Supported by NIH National Research Service Award Postdoctoral Fellowship 5F32CA110636.

[2] Current address: Raybiotech Inc., Norcross, GA 30092.

[3] To whom correspondence should be addressed: Life Sciences Inst. and Dept. of Medicinal Chemistry, University of Michigan, 210 Washtenaw Ave., Ann Arbor, MI 48109-2216. Tel.: 734-615-3129; Fax: 734-615-9907; E-mail: davidhs@lsi.umich.edu.

[4] The abbreviations used are: MC, mitomycin C; MA, mitomycin A; ME, mitomycin E; MB, mitomycin B; AdoMet, *S*-adenosyl-L-methionine; HR-CIMS, high-resolution chemical ionization mass spectrometry; HPLC, high-pressure liquid chromatography; TLC, thin-layer chromatography; HMBC, heteronuclear multiple-band correlation; GOESY, gradient-enhanced nuclear Overhauser effect spectroscopy.

mectin (AveD: 37% identity, 52% similarity (23, 24)), monensin (MonE: 34% identity, 51% similarity (25)), and rifamycin (ORF14: 33% identity, 50% similarity (26)). Therefore, we initially hypothesized that MitM and MitN are involved in C-9a side chain methylation for mitomycin biosynthesis. Our previous studies had shown that a *mitM* deletion mutant was blocked in MA and MC production but accumulated mitomycin B (MB) and a new mitomycin analog, 9a-demethylmitomycin A (**6**) (27). Interestingly, the conversion of 9a-demethyl-MA by MitM in the presence of AdoMet resulted in 9-*epi*-mitomycin B (**7**) instead of the expected MA, demonstrating that MitM functions as an aziridine *N*-methyltransferase (27) that acts on the 9β series of mitomycins.

Here we describe studies on a *mitN* in-frame deletion mutant as part of a continuing effort to investigate the role of methyltransferases in the late stages of the mitomycin pathway. The *mitN* mutant strain of *S. lavendulae* was unable to produce MB and accumulated a new mitomycin analogue, 9-*epi*-mitomycin C (**10**). The production of MC and MA was unaffected by the deletion of *mitN*. In the presence of MitN and AdoMet, 9-*epi*-MC was converted to a new product, mitomycin E (**12**). These results show that MitN is also an aziridine *N*-methyltransferase that is involved in tailoring of the 9α-series of mitomycins.

EXPERIMENTAL PROCEDURES

General Procedures—NMR spectra were recorded on a Varian INOVA 500 spectrometer operating at 500 MHz for ^{1}H and 125 MHz for ^{13}C, using solvent signals as internal references. High-resolution (HR) and low-resolution (LR) chemical ionization mass spectrometry (CIMS) of 9-*epi*-MC were measured on a Finnigan MAT 90/95 sector-field mass spectrometer, and HR-CIMS of ME was measured on a Micromass ZAB-SE mass spectrometer. IR spectra were obtained on a PerkinElmer 1600 series Fourier-transformed infrared (FT-IR) spectrophotometer. The optical rotations were measured on a Jasco DIP-370 digital polarimeter. The concentration of MitN was determined with a Beckman DU640 UV spectrophotometer. A Beckman Coulter System Gold autosampler, pump, and photodiode array detector were used in the HPLC separation and analyses.

Materials—All solvents were of HPLC grade and were used without further purification. *S. lavendulae* NRRL 2564 was used as the source strain for creation of gene disruption mutants. Analytical thin-layer chromatography (TLC) was carried out on Merck silica gel G-254 plates.

Chromatography—The isolation of 9-*epi*-MC and the conversion reactions were monitored by TLC using Merck silica gel 60F-254 aluminum sheets. TLC plates were developed in 10% methanol in chloroform. Column chromatography was performed on 32–63-μm particle size silica gel (Scientific Absorbents Inc.). Final purification of 9-*epi*-MC and MitN enzyme kinetic analyses was accomplished using HPLC (Alltech Econosil C_{18}; 250 $\times$ 4.6 mm, 5 μm; 20–60% aqueous methanol in 20 min, 60% for 4 min, and 60–100% in 2 min at 1 ml/min; monitored at 313 and 360 nm).

Bacterial Strains and Cloning Vectors—*Escherichia coli* DH5α was routinely used as a cloning host and was propagated on LB medium. *E. coli* S17-1 was used as a conjugation host for gene transfer from *E. coli* to *S. lavendulae*. Conjugation was performed using AS1 medium, and chromosomal double crossover recombination was selected on R5 media as described previously (28). *E. coli* BL21(DE3) was the protein overexpression host in NZCYM media. pUC119 was the cloning vector in *E. coli*, and the *E. coli-Streptomyces* conjugative shuttle vector pKC1139 was used to create disruption mutants in *S. lavendulae*. pET28b was used for protein overexpression in *E. coli* BL21(DE3).

Creation of MitN Disruption Mutant of S. lavendulae—The *mitN* in-frame deletion mutant was constructed in a two-step process. In the first step, a *mitM* insertional disruption mutant bearing the kanamycin resistance gene was created (MM106) (29). To generate this mutant, the pUC119-based plasmid bearing *mitM* and *mitN* (pDHS7608) was digested with Bpu11021, which cuts *mitM*, and then blunt-ended. This vector was ligated with a 1.4-kb ApaL1-HindIII fragment (*aphII*) from pFD666 (30) to create pDHS7705. The insertion of the *aphII* gene in the Bpu11021 site results in the disruption of *mitM* as well as kanamycin resistance. The 3.9-kb BamHI insert was cloned into the shuttle vector pKC1139 to generate pDHS7706.

In the next step, the *mitN* in-frame deletion mutant construct was generated. A 1.9-kb *mitN* upstream fragment (MTF12) and a 1.3-kb downstream fragment (MTF33) were amplified with two pairs of primers: primer f1 (5′-GC TCT AGA TCT ACG TCT CCC GCG-3′ (XbaI)) and primer r2 (5′-GC CTC GAG CGT CAT GCC GCT CAC TTT-3′ (XhoI)) for MTF12 and primer f3 (5′-GC CTC GAG TAG GGC TCC CAC GGG AGG-3′ (XhoI)) and primer r3 (5′-GC AAG CTT CGG CAT CAC GCG CCA-3′ (HindIII)) for MTF33. MTF12, the *mitN* upstream fragment, contains the nonmutated version of *mitM*. Three-way ligation of the XbaI/XhoI-digested MTF12, XhoI/HindIII-digested MTF33, and the XbaI/HindIII-digested pUC119 resulted in pDHS7709, in which a nondisrupted version of *mitM* was in its original orientation to the start of *mitN* and *mitN* was replaced with a XhoI site. pDHS7710 was created by subcloning the 3.2-kb XbaI/HindIII inserted from pDHS7709 into pKC1139.

A two-step recombination strategy was used to create the *mitN* in-frame deletion mutant DHS5373. First, the *mitM* insertional mutant (MM106) was created by conjugating the disruption mutant pDHS7706 into the wild-type *S. lavendulae* NRRL 2564 according to the methods described previously (28, 29). Transconjugates that were both apramycin- and kanamycin-resistant were selected on AS1 plates (31), overlaid with apramycin, kanamycin, and nalidixic acid, and propagated on R5T plates (32) at 39 °C for several generations. As the origin of the shuttle vector is temperature-sensitive, the presence of the insertional disruption on the chromosome was monitored by the phenotype shifting from both apramycin- and kanamycin-resistant to apramycin-sensitive and kanamycin-resistant. Southern blot hybridizations were used to verify the genotype of the insertional mutant (data not shown).

The *mitN* deletion mutant (DHS5373) was created by conjugating pDHS7710 into MM106, the *mitM* insertional mutant (29). Deletion mutants were screened for phenotype change from apramycin- and kanamycin-resistant to apramycin- and kanamycin-sensitive. In this mutant, *mitN* was deleted from the chromosome, and the nondisrupted *mitM* was restored. Dele-

tion of *mitN* in DHS5373 was confirmed by Southern blot hybridization (data not shown).

Cloning, Overexpression, and Purification of MitN—For the construction of the *mitN* overexpression vector, an NdeI site was introduced at the translational start codon of *mitN* with primer f5 (5′-GTG AGC CAT ATG ACG GAA ACC GCG TCC GC-3′ (NdeI)). With pDHS7608 containing the *mitMN* genes as template and M13/pUC reverse sequencing primer as the other PCR primer pair, a 1.45-kb fragment was amplified. The resulting fragments were digested with NdeI-HindIII and subcloned into the corresponding sites of pET28b to generate pDHS5155. The overexpressed proteins were engineered to include an N-terminal His_6 tag.

pDHS5515 was transformed into the *E. coli* BL21(DE3) strain for overexpression of MitN. *E. coli* was grown at 37 °C in NZCYM broth containing 50 μl/ml kanamycin until $A_{600} = 0.6$. Expression of MitN was induced by adding isopropyl 1-thio-β-D-galactopyranoside to a final concentration of 0.1 mM and reducing the temperature to 25 °C. After incubating the culture overnight, cells were harvested, suspended in ice-cold buffer (50 mM NaH_2PO_4, pH 8.0, 300 mM NaCl, 10 mM imidazole), and lysed by sonication (6 × 10 s with 10-s pauses at 200–300 watts). The supernatant collected by centrifuging the lysate at 10,000 × *g* at 4 °C was applied to a Qiagen nickel-nitrilotriacetic acid column. The column was washed twice with wash buffer (50 mM NaH_2PO_4, pH 8.0, 300 mM NaCl, 20 mM imidazole) followed by dissolving the protein in elution buffer (50 mM NaH_2PO_4, pH 8.0, 300 mM NaCl, 250 imidazole). The eluent was desalted by passing it through a PD-10 column (Amersham Biosciences), and eluted in 50 mM potassium buffer, pH 7.4. MitN was further concentrated on an Amicon Ultra 10-kDa centrifugal device. The protein concentration was determined by Bradford assay using bovine serum albumin as the standard. The final concentration of MitN was 190 μM (6.1 mg/ml). Protein size was estimated by analytical gel filtration (Sephadex 200) on an Akta FPLC (Amersham Biosciences).

Enzyme Assays—Enzymatic conversion of MitN with 9-*epi*-MC and MA was carried out in a total volume of 50 μl in 50 mM sodium phosphate buffer, pH 7.4, containing 200 μM AdoMet, an appropriate quantity of substrate, and 1 μM purified enzyme. The reactions were incubated at 30 °C for 30 min and were terminated by being extracted twice with an equal volume of ethyl acetate. The combined organic extracts were dried under a stream of nitrogen, resuspended in 40 μl of methanol, and subjected to TLC and HPLC analysis. New products from several standard enzymatic reactions were isolated and purified by reverse phase HPLC and subjected to NMR and mass spectral analyses. For kinetic analyses, conversion was measured by analytical HPLC. Preliminary experiments determined the parameters of initial rates of conversion, and these conditions were used to determine kinetic values of MitN with MA, 9-*epi*-MC, and AdoMet. Samples were run in triplicate. Curves were fitted using Prism3 software (GraphPad Software, Inc.).

The ability of divalent cations to enhance the conversion of MA to MF by MitN was assessed. Reactions were performed in duplicate under the same conditions as described previously but with the addition of 1 mM EDTA, Ca^{2+}, Cu^{2+}, Mg^{2+}, Mn^{2+}, or Zn^{2+}. The final concentrations of AdoMet and MA were 200 and 250 μM, respectively. 9-*epi*-MC was not used as a substrate because of the small amount of material available.

Fermentation Conditions—The *mitN* mutant (DHS5373) of *S. lavendulae* was grown on R2YE agar medium for 7 days. A single colony was selected, inoculated into 50 ml of seed medium (tryptic soy broth), and grown at 30 °C with vigorous shaking (250 rpm). After 48 h, 500 μl of the seed medium was inoculated into 500 ml of the production culture (Nishikohri medium) (33) and grown under the same conditions for 96 h.

Metabolite Isolation—The fermentation broth was centrifuged at 3000 rpm for 10 min and the supernatant extracted twice with ethyl acetate. The combined organic extract was dried *in vacuo* to yield a tart brown oil. Crude extract was dissolved in methanol and loaded on a Sephadex LH-20 column (2.5 × 120 cm, methanol). MA was eluted first followed by 9-*epi*-MC and MC, respectively. The eluted fractions were combined based on the TLC profiles. The combined fraction that contained 9-*epi*-MC was further purified by silica gel column chromatography using a stepped gradient elution (2% MeOH/$CHCl_3$ to 50% MeOH/$CHCl_3$) followed by reverse phase HPLC to afford 9-*epi*-MC. The fractions containing MA and MC were purified in a similar fashion to yield 0.23 mg/liter MA and 4.93 mg/liter MC. The structure of MA was confirmed by comparison of the ^1H NMR and mass spectral data with an authentic sample.

RESULTS

Creation of a mitN Deletion Mutant—A *mitN* deletion mutant (DHS5373) was created from the *S. lavendulae mitM* insertional mutant strain MM106 (29). The mutants were screened for phenotype change from kanamycin, apramycin double resistant to double sensitive, and confirmed by the correct band shift with Southern blot hybridization (data not shown). DHS5373 had identical growth characteristics as wild-type *S.-lavendulae*. The two-dimensional TLC analysis of the crude extract showed production of MC (**3**), MA (**1**), and a new purple-pigmented compound. Interestingly, MB (**8**), which is typically produced by the *S. lavendulae* wild-type strain cultured under the same growth conditions, was not observed in the extract of DHS5373.

Isolation and Structure Elucidation of a New Mitomycin Intermediate—To identify the structure of the accumulated intermediate, DHS5373 was fermented in 6 liters of Nishikohri medium (33). After 96 h, the fermentation broth was centrifuged, and the supernatant was extracted twice with ethyl acetate. The organic extract was combined and dried *in vacuo* to yield a brown oil (652 mg). The crude extract was subjected to gel permeation (LH-20) column chromatography using methanol as the eluent. MA (**1**) eluted first followed by the newly accumulated intermediate 9-*epi*-MC (**10**) and MC (**3**), respectively. The fractions that contained compound 9-*epi*-MC were combined, concentrated, and applied to a silica gel column chromatography followed by reverse phase HPLC to afford 0.65 mg/liter 9-*epi*-MC. For the MA- and MC-containing fractions, the purification was performed in a similar fashion to provide MA (0.23 mg/liter)

TABLE 1

NMR spectral data for 9-*epi*-mitomycin C and mitomycin C in Me_2SO-d_6

All ^1H and ^{13}C chemical shifts were referenced to residue natural abundance Me_2SO (δ 2.50 and δ 39.51).

C/H no.	9-*epi*-Mitomycin C			Mitomycin C	
	δ_C[a]	δ_H[b,c]	HMBC[d]	δ_C[a]	δ_H[a,c]
1	36.40	2.66 d (4.5)	H-3	35.35	2.79 d (5.1)
2	34.62	2.90 br d (4.5)	H-3	31.47	2.70 br d (5.1)
3	50.85	3.58 d (12.3) 3.74 d (12.3)		49.13	Overlapped with OCH_3
5	176.99		H-6a	176.90	
5a	155.50		H-3	155.18	
6	102.83		H-6a	102.60	
6a	8.18	1.66 s		8.28	1.66 s
7	149.50		H-6a	148.92	
8	175.27			175.21	
8a	110.57			109.09	
9	44.77	3.63 dd (10.2, 3.3)		40.34	4.01 br d (10.2)
9a	103.82		H-1, H-10, OCH_3	105.75	
10	59.24	4.09 dd (10.5, 3.3) 4.64 t (10.5)		60.87	4.09 t (10.2) 4.56 dd (10.2, 3.9)
10a	157.08		H-10	156.51	
OCH_3	50.70	3.31 s		49.60	3.10 s

[a] Recorded at 75 MHz.
[b] Recorded at 500 MHz.
[c] Numbers in parentheses = *J* in Hz.
[d] Carbons showing long-range correlation with indicated protons.

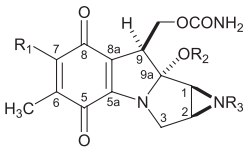

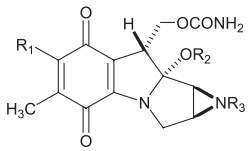

Compound	R_1	R_2	R_3
Mitomycin A (MA, **1**)	OCH_3	CH_3	H
Mitomycin F (MF, **2**)	OCH_3	CH_3	CH_3
Mitomycin C (MC, **3**)	NH_2	CH_3	H
Porfiromycin (**4**)	NH_2	CH_3	CH_3
7-Demethyl-MA (**5**)	OH	CH_3	H
9a-Demethyl-MA (**6**)	OCH_3	H	H
9-*Epi*-MB (**7**)	OCH_3	H	CH_3

Compound	R_1	R_2	R_3
Mitomycin B (MB, **8**)	OCH_3	H	CH_3
7-Demethyl-MB (**9**)	OH	H	CH_3
9-*Epi*-MC (**10**)	NH_2	CH_3	H
Mitomycin D (MD, **11**)	NH_2	H	CH_3
Mitomycin E (ME, **12**)	NH_2	CH_3	CH_3
Mitomycin J (MJ, **13**)	OCH_3	CH_3	CH_3
Mitomycin L (ML, **14**)	$NHCH_3$	H	CH_3

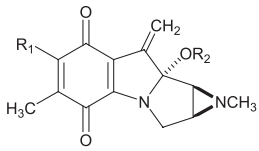

Compound	R_1	R_2
Mitomycin G (MG, **15**)	NH_2	CH_3
Mitomycin H (MH, **16**)	OCH_3	H
Mitomycin K (MK, **17**)	OCH_3	CH_3

FIGURE 1. **Mitomycins isolated from wild-type and mutant strains of *S. lavendulae*.**

and MC (4.93 mg/liter). The structures of both MA and MC were confirmed by comparing the corresponding ^1H NMR spectra with authentic materials.

The HR-CIMS data of 9-*epi*-MC provided a molecular ion peak $(M + H)^+$ at *m/z* 335.1346, which suggested a molecular formula of $C_{15}H_{18}N_4O_5$ and nine double bond equivalents. The ^1H and ^{13}C NMR spectra of 9-*epi*-MC (Table 1) provided a data set similar to that of MC, with the large chemical shift difference observed for protons and carbons at positions 1, 2, 9, and the methoxy group. The connectivities of the carbon and hydrogen atoms of 9-*epi*-MC were confirmed to be identical to that of MC by the interpretation of HMBC spectral data (Table 1). With respect to stereochemistry, C-1, C-2, and C-9a of 9-*epi*-MC were assigned as depicted in Fig. 1 based on biosynthetic correlation with all other naturally occurring mitomycins (34). Because 9-*epi*-MC possesses physical properties that are unique compared with MC (*i.e.* NMR spectral data and R_f value), we proposed it to be a diastereomer possessing the 9α- instead of 9β-carbamoyloxymethyl configuration. To substantiate further the proposed structure of 9-*epi*-MC, the stereochemistry for the C-9—C-10 bond was determined by GOESY experiments. Irradiation of OCH_3 (C-9a, δ 3.31) resulted in enhancements of H-3 (δ3.58) and H-10′ (δ4.64). Although no direct result was observed on H-9, these data clearly suggested that H-1, H-3, H-10′, and OCH_3 protons lie in the same plane, whereas H-9 does not. Hence, the results from the GOESY experiments further confirmed the α-configuration of C-9 of 9-*epi*-MC.

Overexpression and Purification of MitN—The MitN gene product is predicted to be an acidic protein (pI = 4.59) that consists of 275 amino acids with a calculated molecular mass of ~30 kDa. To determine the role of MitN in the biosynthesis of the mitomycins, the protein was overexpressed in *E. coli* BL21(DE3). Production of MitN in the soluble form was achieved by adding very low concentrations of isopropyl 1-thio-β-D-galactopyranoside (0.1 mM), and the protein was purified to homogeneity using

nickel-nitrilotriacetic acid (supplemental Fig. 1). Purified MitN protein was shown by gel filtration chromatography to have a molecular mass of ~32 kDa, suggesting that it exists in solution as a monomer (data not shown).

*MitN Converts 9-epi-MC (**10**) to Mitomycin E (**12**)*—The disruption of *mitN* resulted in production of MA and MC (slight increase in production level, 3.0 mg/liter in the wild-type *S. lavendulae*, 4.93 mg/liter in DHS5373) with accumulation of 9-*epi*-MC. Interestingly, MB, which was found in the wild-type extract cultured under the same conditions, was not observed in the DHS5373 extract. This result indicates that MitN is unlikely to be involved in the biosynthesis of MA and MC but is essential to the biosynthesis of MB. To probe the role of MitN in the mitomycin biosynthetic pathway, compound 9-*epi*-MC was used as a substrate for MitN in the presence of AdoMet. As a result, the enzymatic reaction yielded another purple compound with a higher R_f value by TLC analysis. To identify the structure of this newly formed product, the ethyl acetate extract from the reaction was subjected to reverse phase HPLC and subsequent NMR and mass spectral analyses.

The HR-CIMS measurement of the conversion product ME provided a *m/z* $[M + Na]^+$ 371.1331 analyzing for a molecular formula of $C_{16}H_{20}N_4O_5$, which contains one more carbon and two additional protons compared with 9-*epi*-MC. The ^{1}H NMR spectrum of ME revealed a methyl proton signal at δ 2.27 (supplemental Table 1) that was absent in the ^{1}H NMR spectrum of 9-*epi*-MC. This methyl group was placed on the aziridine nitrogen based on the HMBC correlation observed from C-2 (δ 46.75) to the methyl group at δ 2.22. To confirm the stereochemistry of C9-C10, a GOESY experiment was conducted on ME, which the H-9 signal irradiated and which resulted in the enhancements of H-1 (δ 2.66) and H-10 (δ 4.64) but not OCH_3, providing evidence to support the 9α-carbamoyloxymethyl configuration of ME. Hence, the structure is identified as ME (Fig. 1). ME was previously reported as a natural product with a low production profile, and accompanying spectral data were lacking (5). Therefore, we have included the NMR assignments of ME in supplemental Table 1.

To test further the substrate specificity characteristics of MitN, a series of mitomycin compounds including MA, MB, MC, MD, and MH were investigated as possible substrates for the enzyme. In addition, the ability of MitN to methylate an intermediate isolated from the Δ*mmcR* mutant 7-demethyl-MA (Fig. 1 (19)) was assayed. In the presence of AdoMet and MitN, only MA was converted to a new product, but no products were observed for the other mitomycins tested using the same reaction conditions. The MA conversion product was shown to be MF (Fig. 1) by TLC, HPLC, and ^{1}H NMR analysis in comparison with an authentic standard. MF is identical to MA but carries an additional methyl group attached to the aziridine nitrogen. Thus, the conversion experiments with 9-*epi*-MC and MA suggest that MitN acts as an *N*-methyltransferase.

The MitN apparent kinetic parameters (Fig. 2, Table 2) indicate that 9-*epi*-MC is a preferred substrate compared with MA by MitN. The apparent kinetic parameters of AdoMet are not affected by the mitomycin substrate present. In addition, the rates are fairly slow, similar to the rates of other methyltransferases involved in secondary metabolite modification (19, 35–37).

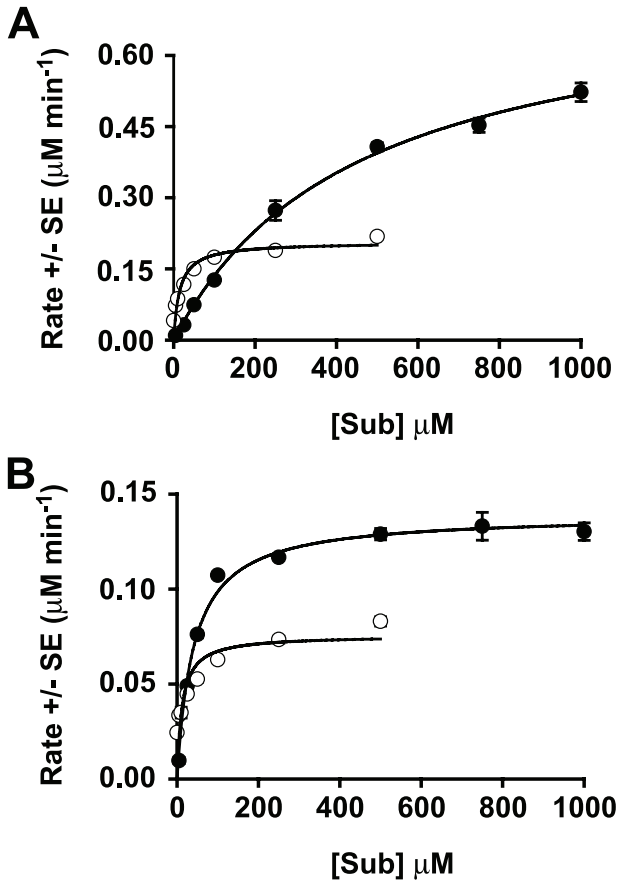

FIGURE 2. **Kinetic data of MitN with AdoMet and mitomycin A (*A*) and 9-*epi*-mitomycin C (*B*).** *Closed circles* represent rates at varying concentrations of either MA (*A*) or 9-*epi*-MC (*B*) with saturating concentration of AdoMet. *Open circles* represent rates at varying concentrations of AdoMet with saturating concentrations of MA and 9-*epi*-MC.

TABLE 2

Kinetic parameters for MitN with mitomycins and AdoMet

The compounds in parentheses are held at saturating concentrations for kinetic parameter determination. Saturating conditions for MA were not met.

Substrate	K_m	V_{max}
	μM	μM min^{-1}
AdoMet (MA)	14.9 ± 2.7	0.206 ± 0.008
9-*epi*-MC (AdoMet)	41.2 ± 3.6	0.139 ± 0.003
AdoMet (9-*epi*-MC)	11.9 ± 3.2	0.076 ± 0.004

The conversion of MA to MF by MitN was not enhanced by the addition of the divalent cations Mg^{2+}, Mn^{2+}, or Ca^{2+} but was inhibited by the addition of Zn^{2+} and Cu^{2+} (Fig. 3). In addition, conversion was not inhibited by the addition of EDTA. Although some AdoMet-dependent methyltransferases require the addition of a divalent cations (38–41), it has been shown that they are not required for several other methyltransferases (19, 42).

*9-epi-Mitomycin C (**10**)*—9-*epi*-MC is a dark purple solid: $[\alpha]^{22}_D = +30.3°$ [*c*, MeOH]; UV (MeOH) λ_{max} (logϵ) 359 (5.36), 240 (5.04) nm; IR (film) ν_{max} 3316, 1595, 1530, 1345, 1060 cm^{-1}. For ^{1}H NMR, ^{13}C NMR, and HMBC data, see Table 1. CIMS: *m/z* (%) 335 $[M + H]^+$ (2), 294 (5), 292 (6), 262 (12), 248 (11), 246 (22), 244 (15), 234 (16), 232 (64), 230 (100), 215 (31),

190 (10), 137 (46). HR-CIMS $[M + H]^+$ *m/z* 335.1346 ($C_{15}H_{19}N_4O_5$, Δ + 1.0 milli mass unit of calculated value).

DISCUSSION

Through identification and sequence analysis of the mitomycin biosynthetic gene cluster, we assigned the product of *mitN* to be a putative AdoMet-dependent methyltransferase (16). To investigate the role of MitN in mitomycin biosynthesis, a *mitN* in-frame deletion mutant (DHS5373) was generated. Surprisingly, the lack of a functional *mitN* gene within the gene cluster did not result in abrogation of MC and MA production. Instead, analysis of the metabolite profile from the DHS5373 extract revealed that production of MB was blocked, and a new mitomycin analog, 9-*epi*-MC, accumulated. Therefore, it appears that MitN is not essential for the generation of MA and MC. In addition, our findings suggest that MitN plays an important role in the biosynthetic pathway of the 9α-carbamoyloxymethyl series of mitomycins.

The conversion of 9-*epi*-MC to ME by MitN in the presence of AdoMet indicated that the enzyme functions as an aziridine *N*-methyltransferase. The MitN enzymatic activity was further confirmed by its conversion of MA to MF, whereas no reaction was observed when MB, MC, MD, MG, and MH were used as substrates. Based on these observations, the substrate specificity of MitN is determined by the stereochemistry at C-9 and by the substituent at C-7. This is most clearly demonstrated by the inability of MitN to use the C-9β-configured MC as a substrate, but the conversion of the C-9α-configured 9-*epi*-MC to give the corresponding *N*-methyl derivative. MA, which differs from MC only in the nature of the C-7 substituent, can serve as a substrate. MB, MD, MG, and MH all carry aziridine *N*-methyl groups and are not substrates for MitN. Taken together, MitN shows a clear preference for the C-9α-configured mitomycins and for C-7-methoxy substituents. Furthermore, MitN acts as an aziridine *N*-methyltransferase *in vitro* and *in vivo*.

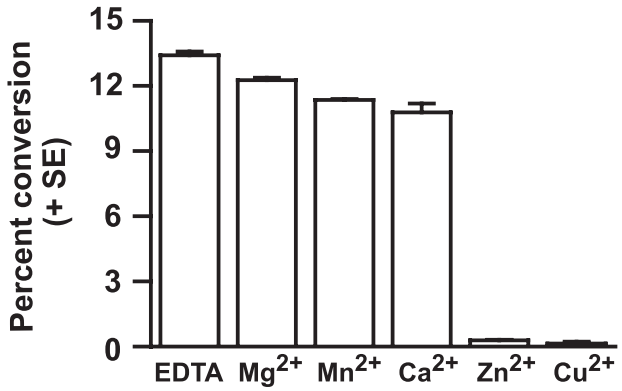

FIGURE 3. **Conversion of MA to MF by MitN in the presence of either EDTA or selected divalent cations.**

Even though 9-*epi*-MC is a good substrate for MitN *in vitro* with an apparent K_m value comparable with that of other methyltransferases (19, 35, 36, 42, 43), it does not yield the isolated natural product MB. Based on examination of the late stage tailoring reactions of mitomycins that possess the 9α-configuration, a new parallel pathway can be proposed based on the results in this study (Fig. 4). As shown in Fig. 1, all of the previously reported mitomycins that possess the 9α-configuration are methylated at N-1a of the aziridine ring. Moreover, because MitN is an aziridine *N*-methyltransferase, we suggest that the actual substrate for MitN is proposed intermediate **20** (Fig. 4), which could arise from an epimerization of C-9 of 9a-demethyl-MA or of intermediate **19**. Although neither intermediate **19** nor **20** has been isolated from any of the mitomycin biosynthetic gene cluster mutants generated to date, 7-demethyl-MB, which differs from intermediate **19** only by the presence of the aziridine methyl group, has been isolated recently from the MmcR deletion mutant (19). One possible reason that we were unable to isolate intermediates **19** and **20** is the instability of the molecules due to the lack of methyl groups. MB, potentially a conversion product from intermediate **20** by MitN, could undergo subsequent transamination at C-7 and *O*-methylation at C9a to yield MD and ME, respectively. Another possibility that cannot be excluded at this point is a biosynthetic route to MB that involves the conversion of 9-*epi*-MC to MF followed by a demethylation at the C-9 position. However, this seems to be

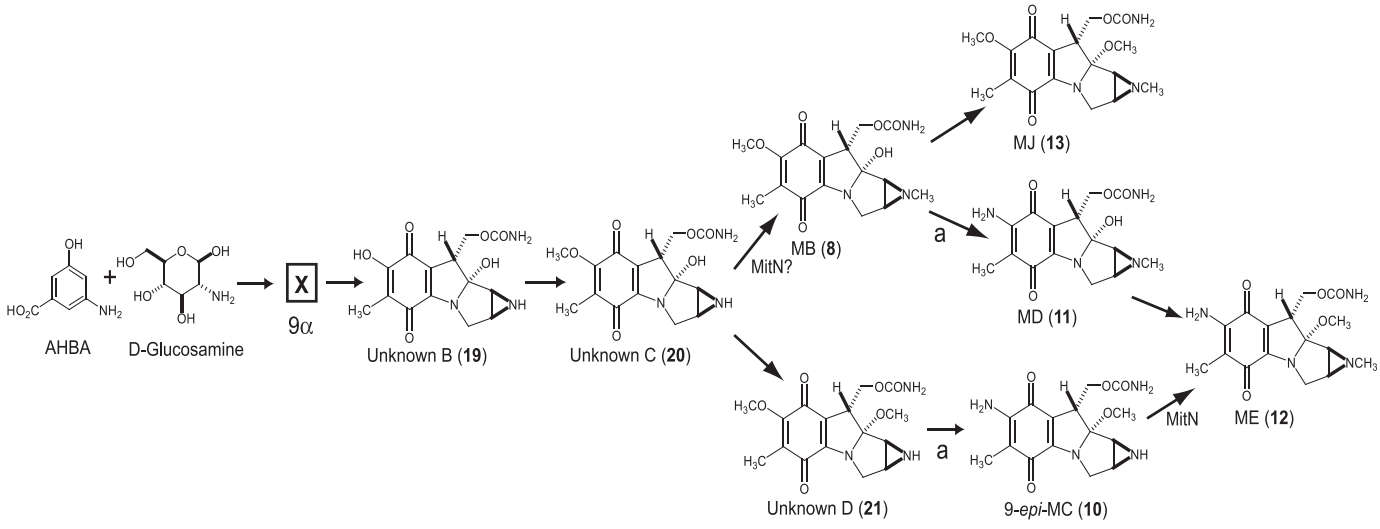

FIGURE 4. **Proposed late stage modifications of 9α branch of mitomycins.**

a remote possibility. It is conceivable that the enzyme that catalyzed *O*-methylation at C-9a has the flexibility to convert MB to MJ. It is significant that deletion of *mitN* from *S. lavendulae* resulted in disruption of MB production and accumulation of 9-*epi*-MC, which is the first compound in the 9α-configuration mitomycin series lacking a methyl group at N-1a. Hence, we propose that in the absence of MitN, intermediate **20** undergoes subsequent *O*-methylation and transamination to provide 9-*epi*-MC as a metabolic shunt product.

To date, there are three different methyltransferases in the mitomycin gene cluster for which substrate specificity has been investigated: MitM is also an aziridine *N*-methyltransferase (27), and MmcR is an *O*-methyltransferase that methylates the hydroxyquinone of the mitosane skeleton at C-7 (16, 19). Deletion mutants of MmcR led to the isolation of two novel metabolites with the 9α- and 9β-configuration, both of which were substrates for *in vitro* bioassays with MmcR, although the substrate with the 9β-configuration is preferred (19). A novel intermediate with the 9β-configuration was isolated from the MitM deletion mutant, and MitM was able to use both this intermediate and MA as substrates (also with 9β-configuration) with poor efficiency (27).

Considering the late stage series of mitomycin modifications, early investigators had proposed that MA is the natural precursor of MC based on the selection of an MC-nonproducing *S. lavendulae* strain that accumulated MA and MB (2). In this respect, it is likely that the biosynthetic pathway leading to the 9α-configuration group diverges from the biosynthetic pathway of 9β-configuration mitomycins prior to the formation of MA (Fig. 4).

In conclusion, this study has demonstrated that MitN is an aziridine *N*-methyltransferase that plays an important role in the biosynthesis of mitomycins bearing the 9α-configuration. However, despite its functional similarity to MitM, MitN is not involved in the formation of MA and MC. This important distinction clearly indicates the existence of a new metabolic branch that operates in parallel to the 9β series of natural product mitomycins. Remaining in question is the origin of the rare 9-oxo-methylene series of metabolites, which may be a third parallel branch pathway or derive specifically from the 9α or 9β series.

Acknowledgments—We are grateful to Kyowa Hakko Kogyo, Ltd. for the gift of mitomycins. We thank the Mass Spectrometry Laboratory at the University of Illinois, Urbana-Champaign for obtaining the high resolution mass spectrum of ME.

REFERENCES

1. Hata, T., Sano, Y., Sugawara, R., Matsumae, A., Kanamori, K., Shima, T., and Hoshi, T. (1956) *J. Antibiot.* **9,** 141–146
2. Wakaki, K., Huromo, H., Tomioka, K., Shimizu, G., Kato, E., Kamada, H., Kudo, S., and Fujimoto, Y. (1958) *Antibiot. Chemother.* **8,** 228–240
3. Lefemine, D. V., Dann, M., Barbatschi, F., Hausmann, W. K., Zbinovsky, V., Monnikendam, P., Adam, J., and Bohonos, N. (1962) *J. Am. Chem. Soc.* **84,** 3184–3185
4. Morton, G. O., Vanlear, G. E., and Fulmor, W. (1970) *J. Am. Chem. Soc.* **92,** 2588–2590
5. Kono, M., Kasai, M., Shirahata, K., and Morimoto, M. (1990) *J. Antibiot.* **43,** 383–390
6. Tomasz, M. (1995) *Chem. Biol.* **2,** 575–579
7. Carter, S. K., and Crooke, S. T. (1979) *Mitomycin C: Current Status and New Developments*, Academic Press, New York
8. Spanswick, V. J., Cummings, J., and Smyth, J. F. (1998) *Gen. Pharmacol.* **31,** 539–544
9. Bradner, W. T. (2001) *Cancer Treat. Rev.* **27,** 35–50
10. Verweij, J., and Pinedo, H. M. (1990) *Cancer Chemother. Biol. Response Modif.* **11,** 67–73
11. Kasai, M., and Arai, H. (1995) *Expert Opin. Ther. Pat.* **5,** 757–770
12. Anderson, M. G., Kibby, J. J., Rickards, R. W., and Rothschild, J. M. (1980) *J. Chem. Soc. Chem. Commun.* 1277–1278
13. Hornemann, U., Kehrer, J. P., Nunez, C. S., and Ranieri, R. L. (1974) *J. Am. Chem. Soc.* **96,** 320–322
14. Hornemann, U., and Eggert, J. H. (1975) *J. Antibiot.* **28,** 841–843
15. Bezanson, G. S., and Vining, L. C. (1971) *Can. J. Biochem.* **49,** 911–918
16. Mao, Y. Q., Varoglu, M., and Sherman, D. H. (1999) *Chem. Biol.* **6,** 251–263
17. Lacalle, R. A., Ruiz, D., and Jimenez, A. (1991) *Gene* **109,** 55–61
18. Ahlert, J., Shepard, E., Lomovskaya, N., Zazopoulos, E., Staffa, A., Bachmann, B. O., Huang, K. X., Fonstein, L., Czisny, A., Whitwam, R. E., Farnet, C. M., and Thorson, J. S. (2002) *Science* **297,** 1173–1176
19. Grüschow, S., Chang, L. C., Mao, Y., and Sherman, D. H. (2007) *J. Am. Chem. Soc.* **129,** 6470–6476
20. Gao, Q. J., Zhang, C. S., Blanchard, S., and Thorson, J. S. (2006) *Chem. Biol.* **13,** 733–743
21. Nishizawa, T., Aldrich, C. C., and Sherman, D. H. (2005) *J. Bacteriol.* **187,** 2084–2092
22. Zhang, C., Albermann, C., Fu, X., Peters, N. R., Chisholm, J. D., Zhang, G. S., Gilbert, E. J., Wang, P. G., Van Vranken, D. L., and Thorson, J. S. (2006) *Chembiochem* **7,** 795–804
23. Ikeda, H., Nonomiya, T., Usami, M., Ohta, T., and Omura, S. (1999) *Proc. Natl. Acad. Sci. U. S. A.* **96,** 9509–9514
24. Hong, Y. S., Lee, J. H., Kim, H. S., Kim, K. W., and Lee, J. J. (2001) *Biotechnol. Lett.* **23,** 1765–1770
25. Oliynyk, M., Stark, C. B. W., Bhatt, A., Jones, M. A., Hughes-Thomas, Z. A., Wilkinson, C., Oliynyk, Z., Demydchuk, Y., Staunton, J., and Leadlay, P. F. (2003) *Mol. Microbiol.* **49,** 1179–1190
26. August, P. R., Tang, L., Yoon, Y. J., Ning, S., Muller, R., Yu, T. W., Taylor, M., Hoffmann, D., Kim, C. G., Zhang, X. H., Hutchinson, C. R., and Floss, H. G. (1998) *Chem. Biol.* **5,** 69–79
27. Varoglu, M., Mao, Y. Q., and Sherman, D. H. (2001) *J. Am. Chem. Soc.* **123,** 6712–6713
28. Mao, Y. Q., Varoglu, M., and Sherman, D. H. (1999) *J. Bacteriol.* **181,** 2199–2208
29. Mao, Y. (2000) *Molecular and Genetic Analysis of Mitomycin C Biosynthesis in Streptomyces lavendulae.* Ph.D. thesis, p. 191, University of Minnesota, Minneapolis
30. Denis, F., and Brzezinski, R. (1992) *Gene* **111,** 115–118
31. Baltz, R. H. (1980) *Dev. Ind. Microbiol.* **21,** 43–54
32. Mazodier, P., Petter, R., and Thompson, C. (1989) *J. Bacteriol.* **171,** 3583–3585
33. Nishikohri, K., and Fukui, S. (1975) *Eur. J. Appl. Microbiol.* **2,** 129–155
34. Hornemann, U., and Heins, M. J. (1985) *J. Org. Chem.* **50,** 1301–1302
35. Freel Meyers, C. L., Oberthur, M., Xu, H., Heide, L., Kahne, D., and Walsh, C. T. (2004) *Angew. Chem. Int. Ed.* **43,** 67–70
36. Lavid, N., Wang, J. H., Shalit, M., Guterman, I., Bar, E., Beuerle, T., Menda, N., Shafir, S., Zamir, D., Adam, Z., Vainstein, A., Weiss, D., Pichersky, E., and Lewinsohn, E. (2002) *Plant Physiol.* **129,** 1899–1907
37. Pacholec, M., Tao, J. H., and Walsh, T. W. (2005) *Biochemistry* **44,** 14969–14976
38. Kreuzman, A. J., Turner, J. R., and Yeh, W. K. (1988) *J. Biol. Chem.* **263,** 15626–15633
39. Bauer, N. J., Kreuzman, A. J., Dotzlaf, J. E., and Yeh, W. K. (1988) *J. Biol. Chem.* **263,** 15619–15625
40. Dhar, K., and Rosazza, J. P. N. (2000) *Appl. Environ. Microbiol.* **66,** 4877–4882
41. Shafiee, A., Motamedi, H., and Chen, T. (1994) *Eur. J. Biochem.* **225,** 755–764
42. Xu, J., Mahmud, T., and Floss, H. G. (2003) *Arch. Biochem. Biophys.* **411,** 277–288
43. Wang, J. H., and Pichersky, E. (1999) *Arch. Biochem. Biophys.* **368,** 172–180